ASI

Carbon – Science and Technology

ISSN 0974 – 0546

http://www.applied-science-innovations.com

RESEARCH ARTICLE Received:13/09/2015, Accepted:02/10/2015

Air flow investigations in direct type solar food dryer using computational fluid dynamics

Pankaj K. Gupta

Mechanical Engineering Department, Chhatrapati Shivaji Institute of Technology, Durg, Chhattisgarh, 491001, India.

Abstract: Flow and temperature field inside a direct type solar dryer is investigated using Computational Fluid Dynamics (CFD). The coupled field analysis is carried out in ANSYS Fluent 12.0. The effect of location of inlet and outlet vents on the predicted velocity and temperature field of the air inside the dryer is analyzed. It is observed that a more uniform air flow and temperature distributions results for inlet vent location at bottom wall of drying chamber.

Keywords: solar food dryer, CFD, air flow, temperature distribution

1 Introduction: Drying of agriculture food products under open sun has been in existing since humanity. Open sun drying though very economical and cumbersome-free has its own disadvantages in that the food being dried is subject to contaminants, dirt and pollution **[1]**. Solar dryers on the other hand not only keep the food products free from such contaminants, but also maintains the flavour, texture, and nutritional quality. Various designs of solar food dryers are in practice, and they are being continuously analysed for improving their performance. Many researchers **[1, 2]** have devoted time and energy in improving its performance while also trying to make it economical. Yet others **[3]** have envisaged methods to compare and asses the performances of solar dryers based on various other designs.

In the quest for continuous development towards optimizing performance of the solar dryers, it is quickly realized that development and subsequent experimentation on each design with a number of parameters critically affecting the performance is a time, energy and capital consuming task. Computational Fluid Dynamics (CFD) has evolved as a very powerful tool to numerically model and analyze physical models **[4, 5]**. One of its greatest advantages has been in visualizing 'what if' scenarios and obtain detailed information within the computational domain unlike experimentations.

The objective of the present work therefore is to employ CFD in predicting the air flow and temperature distribution within a direct type solar dryer. Solar dryers can be classified into four types **[4]**: (1) direct type dryers where the sun's radiation passing through a transparent glass are allowed to heat the food encased in a chamber whose inner surfaces could be of material capable of absorbing radiation; (2) indirect type dryers are those which employ a solar collector to heat the air outside the drying chamber which is then sent into the chamber; (3) mixed type dryers which is a combination of direct- and indirect-type dryers; and (4) hybrid dryers which has a separate heating unit (usually electrical) along with the solar drying so that in the event of poor or unavailability of sunshine, the backup- heating unit takes over to facilitate drying process. Figure (1) shows the schematic diagram of the four types of solar dryers.

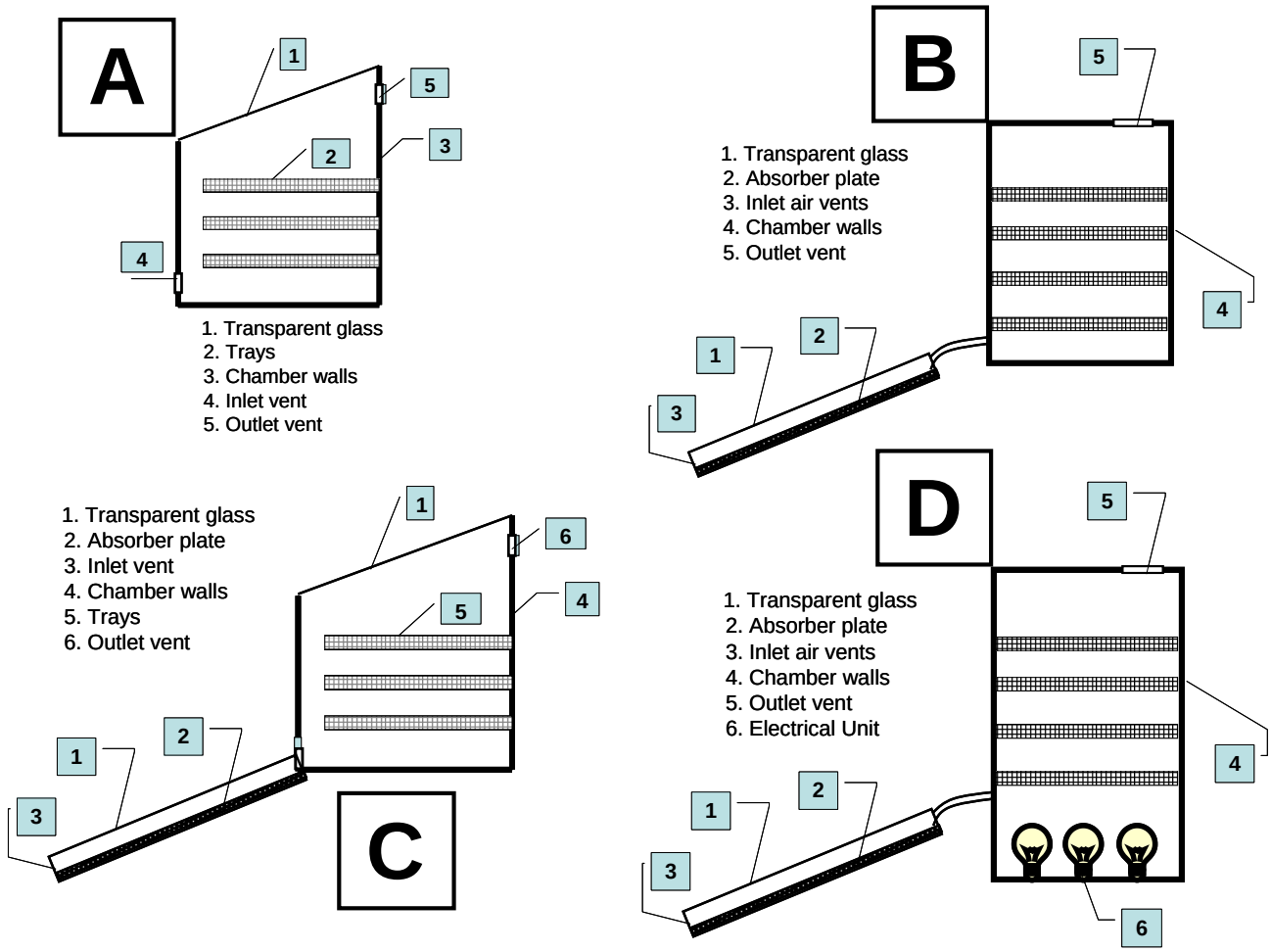

Figure (1): Schematic of (a) Direct solar dryer (b) Indirect solar dryer (c) Mixed solar dryer and (d) Hybrid solar dryer.

The drying process itself is a complex phenomenon **[5]** where momentum, energy and mass transfer takes place. Due to the temperature difference maintained between the food products being dried and the heated air, the moisture (hence mass) present in the food diffuses to the surface of the food and then it is carried away with the air. Thus it can be seen that if there is a quiescent layer of air above the drying product, the air will gradually become saturated with moisture and can no more hold up the moisture. Thus there must be a constant supply of heated air through or above the food being dried.

The supply of fresh air is maintained either by natural convention or by forced convection or by a combination of both **[2]**. Chimney draught is usually employed to facilitate natural convection drying. Forced convection drying is facilitated either by blower or fan.

In the present study, a forced convection direct type solar dryer as shown schematically in Figure (2) is considered. The material for the transparent glass is replaced with an Ultraviolet radiation-resistant material. The use of UV-resistant sheet helps in protecting the food product from ill-effects of UV rays.

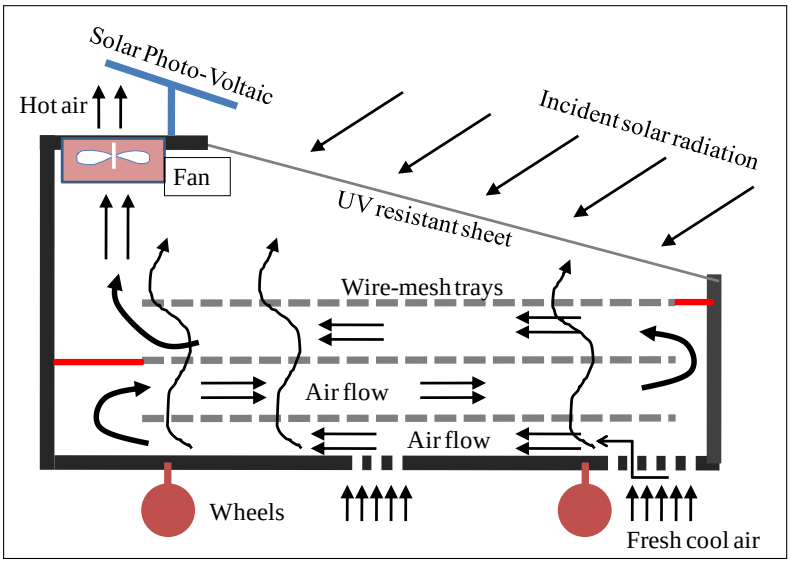

Figure (2): Schematic of forced convection direct solar dryer.

2. Methodology: The numerical modeling of the direct solar dryer is carried out in a two-dimensional plane (the mid-plane of the actual dryer) as shown in Figure (3a). Figure (3b) shows the meshed domain. Two-dimensional assumption could be made if the end-wall effects are neglected **[5]**. The meshing is done in GAMBIT pre-processor and ANSYS FLUENT **[6]** is used for the modeling and post-processing.

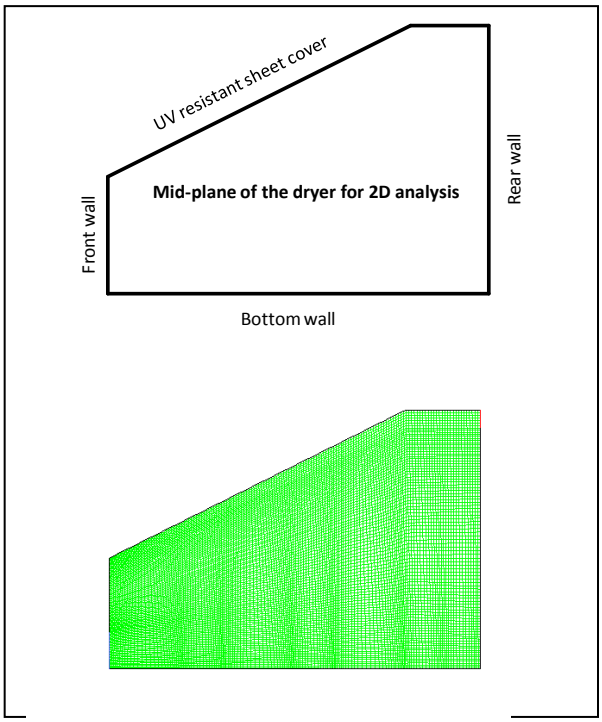

Figure (3): (a) Mid-plane of the dryer for 2D analysis and (b) meshed domain.

The steady state equations governing mass, momentum and energy transfer of the air fluid inside the drying chamber are given by **[6]**

$$\nabla \cdot \left(\rho \vec{U} \right) = 0$$

$$\nabla \cdot \left(\rho \vec{U} \vec{U} \right) = -\nabla p + \nabla \cdot \left[\mu_{eff} \left(\nabla \vec{U} \right) \right] + B$$

and

$$\nabla \cdot \left(\rho \vec{U} h_{tot} \right) = \nabla \cdot \left(k \nabla T \right) + S_E$$

In the above equations, B is the sum of body forces, μ_{eff} is the effective viscosity taking into account for turbulence, and h_{tot} is the total enthalpy given as **[6]**

$$h_{tot} = h + U^2/2$$

Turbulence is modelled using the RNG k-ε model which has been found suitable for mimicking the physics of the present problem. The equations governing turbulent kinetic energy and its rate of dissipation are given as

$$\frac{\partial}{\partial x_i}\left(\rho k U_i \right) = \frac{\partial}{\partial x_i}\left(\alpha_k \mu_{eff} \frac{\partial k}{\partial x_j} \right) + G_k + G_b - \rho \varepsilon - Y_M$$

and

$$\frac{\partial}{\partial x_i}\left(\rho \varepsilon U_i \right) = \frac{\partial}{\partial x_i}\left(\alpha_\varepsilon \mu_{eff} \frac{\partial \varepsilon}{\partial x_j} \right) + C_{1\varepsilon} \frac{\varepsilon}{k}\left(G_k + C_{3\varepsilon} G_b \right) - C_{2\varepsilon} \rho \frac{\varepsilon^2}{k} - R_\varepsilon$$

For the meaning of the various terms in Equations (5-6) and the model constants used, please refer Fluent Manual **[6]**.

One of the objectives of the present study has been to study the effect of location of inlet and outlet vents on the flow field and temperature field of air inside the chamber. The locations of the inlet and outlet vents are varied to evaluate its effect on the flow field. The boundary conditions considered in this study are presented in Table 1.

Table (1) Boundary conditions for the dryer

	Boundary Conditions
Inlet	Velocity inlet
Outlet	Pressure outlet
Glass wall	Constant temperature
Chamber walls	Prescribed temperature

The locations of the inlet and outlet vents are designated as follows. When the inlet and outlet vents are on the front and rear walls of the drying chamber respectively, the configuration is designated as LOC-FR. When the locations of inlet and outlet vents are on the bottom and top walls of the chamber, it is designated as LOC-BT.

3. Results and Discussion:

The results are partially validated against mesh independence using refined meshes. The most economical mesh size was chosen since it reduced the computation time and the results are in good agreement with those from refined meshes.

The run was made on a Pentium Dual core machine with 2.66 GHz processor, 2 GB RAM. The computation times for the three refined meshes are shown in Table 2.

Table (2) Computation time for various meshes

	Cell count	Nodes	Time for computation (in seconds)
Mesh A	9630	9935	135
Mesh B	13724	13973	252
Mesh C	18674	19131	524

Since meshes B and C yield results with an error between them less than 0.2%, Mesh B is retained for all further computations to reduce the time.

Figure (4) shows the temperature distribution in the dryer chamber for LOC-FR configuration. It is observed that the temperature variation is more near the bottom and rear walls of the chamber. This is due to the prescribed temperature boundary conditions at those walls. Such conditions can be taken as an average temperature during certain period of sunshine. In order to get a better understanding of the temperature variations, computations need to be made for different hours of the day, taking the hourly average temperatures prescribed at the boundaries. Such approach has been used in **[7]**.

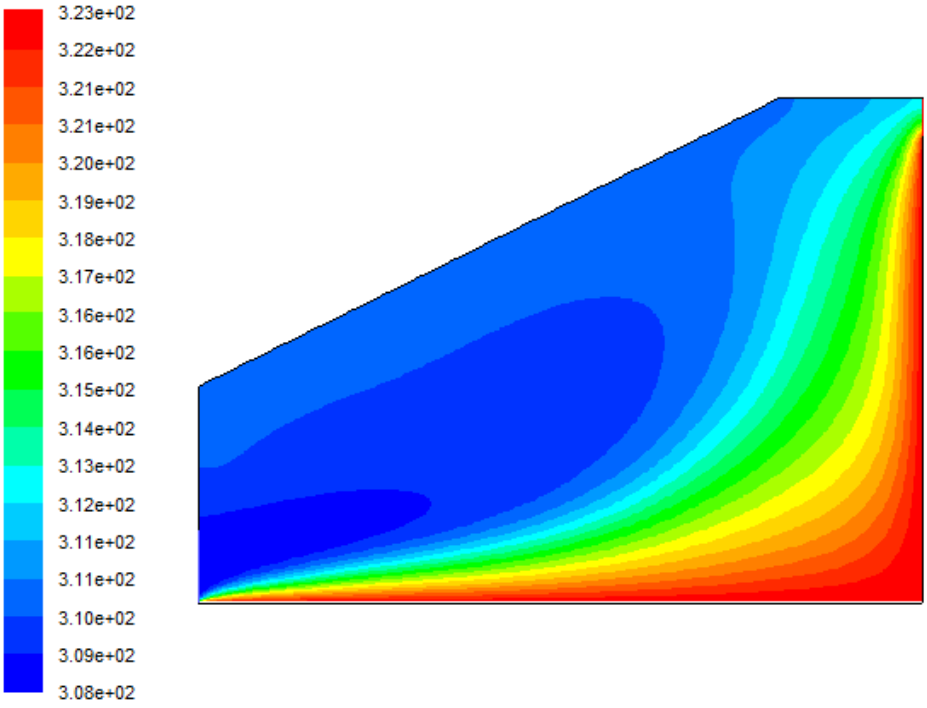

Figure (4): . Temperature distribution for LOC-FR configuration of the dryer.

Figure (5 and 6) show respectively the air flow distribution and velocity vectors in the chamber for LOC-FR configuration. From the figures, it is evident that the corner region (where the rear wall meets the bottom wall) experiences less flow. As the flow inlet is in the Front side of the chamber, air flows towards the outlet (located at top wall). Hence, it is possible that much air is not available at this corner thus affecting the drying if the trays are located from near the rear wall.

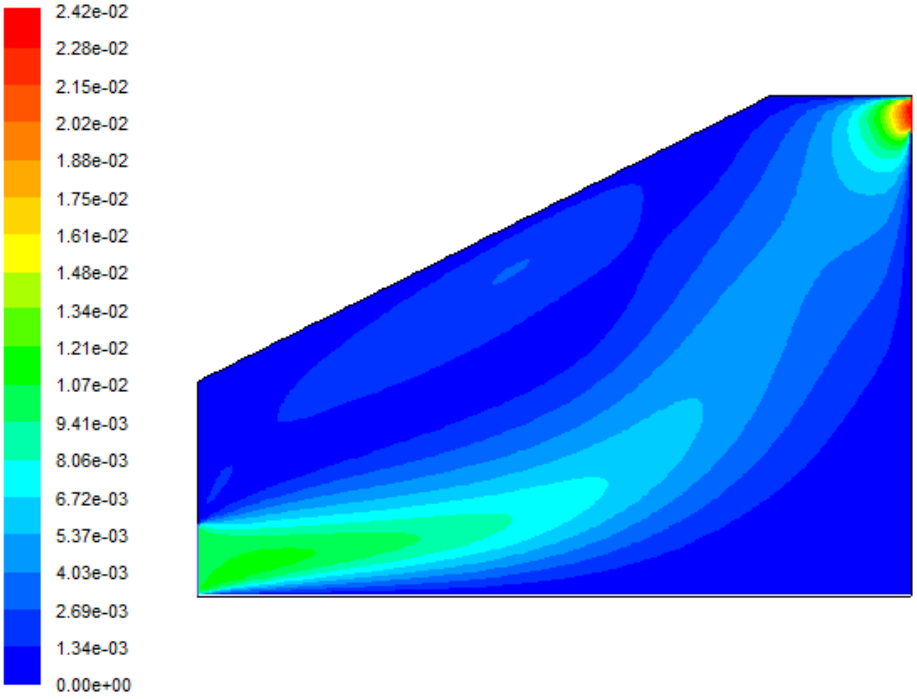

Figure (5): . Air velocity distribution for LOC-FR configuration of the dryer.

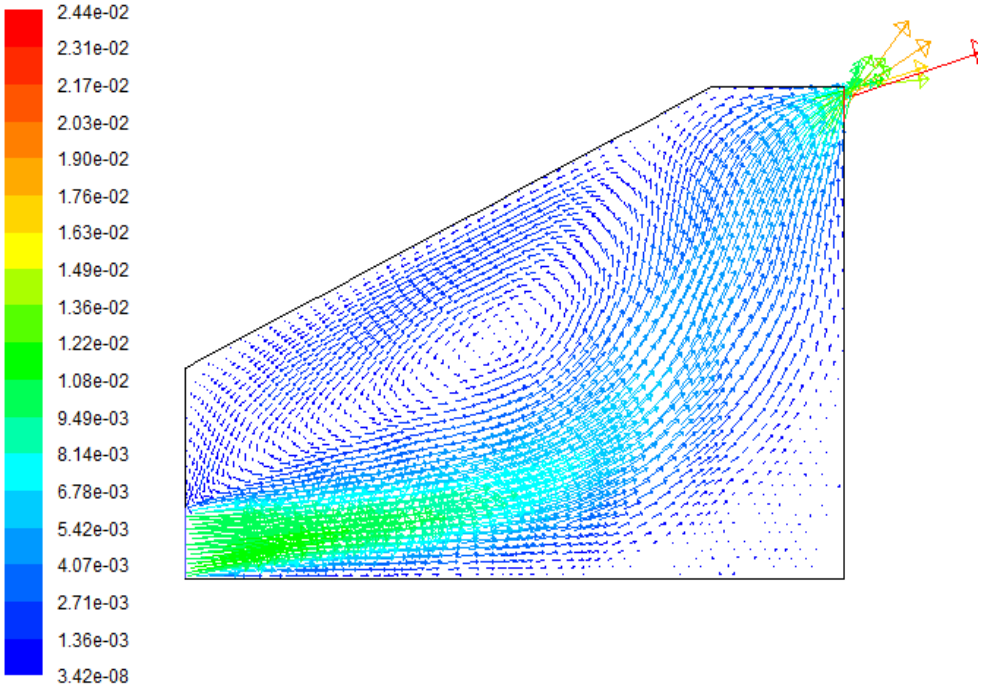

Figure (6): . Veolcity vectors for LOC-FR configuration of the dryer.

Figure (7) shows the distribution of air temperature in the chamber for LOC-BT configuration where the inlet vents are located at the bottom wall of the chamber. From the figure, it can be seen that the air temperature is more uniformly distributed as compared to that in LOC-FR configuration (refer Figure 4). Thus a more uniform drying can be obtained from this configuration.

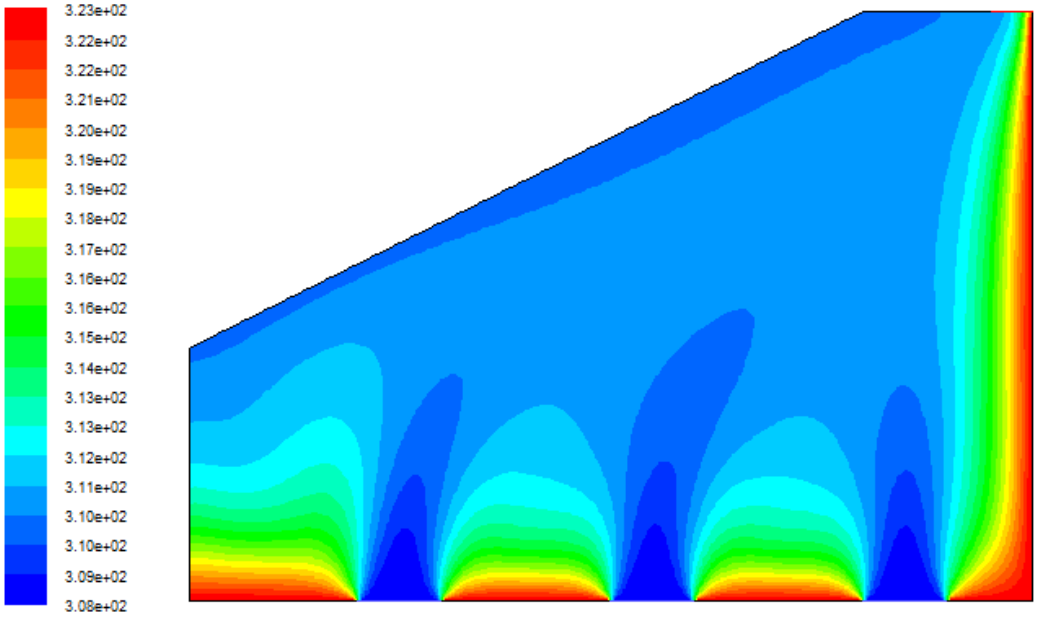

Figure (7): . Temperature distribution for LOC-BT configuration of the dryer.

Figure (8 and 9) shows respectively the air flow distribution and its velocity vectors. Except for the region near the front wall of the chamber, the air flow is more distributed as compared to that in configuration LOC-FR. The corner region (near the rear wall and bottom wall meeting point) also has a better air flow, thus utilizing availability of fresh air for drying, since the trays are located near the rear wall.

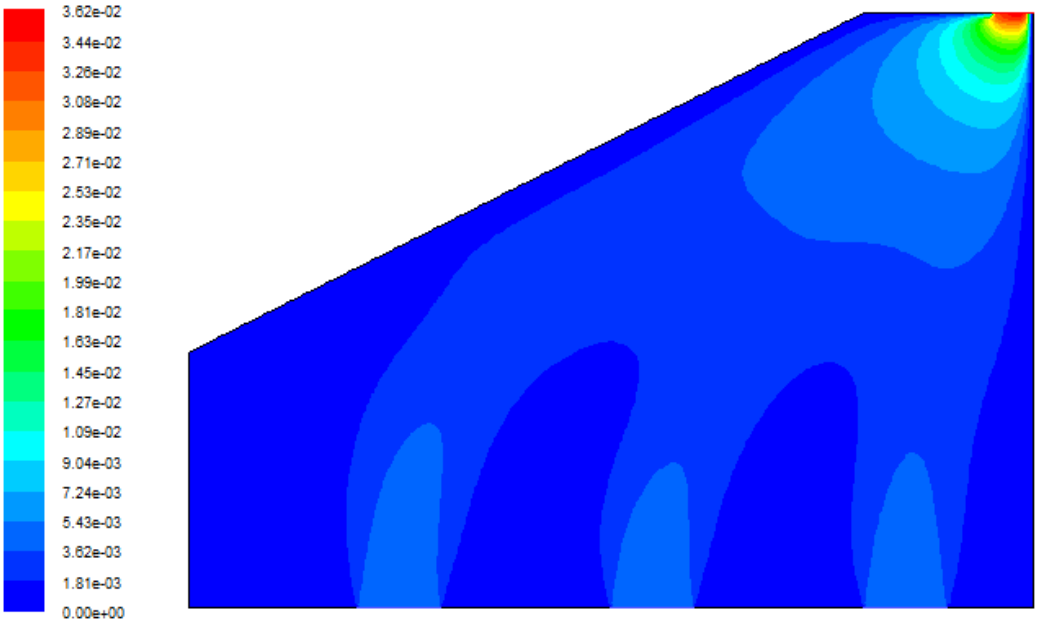

Figure (8): . Air flow distribution for LOC-BT configuration of the dryer.

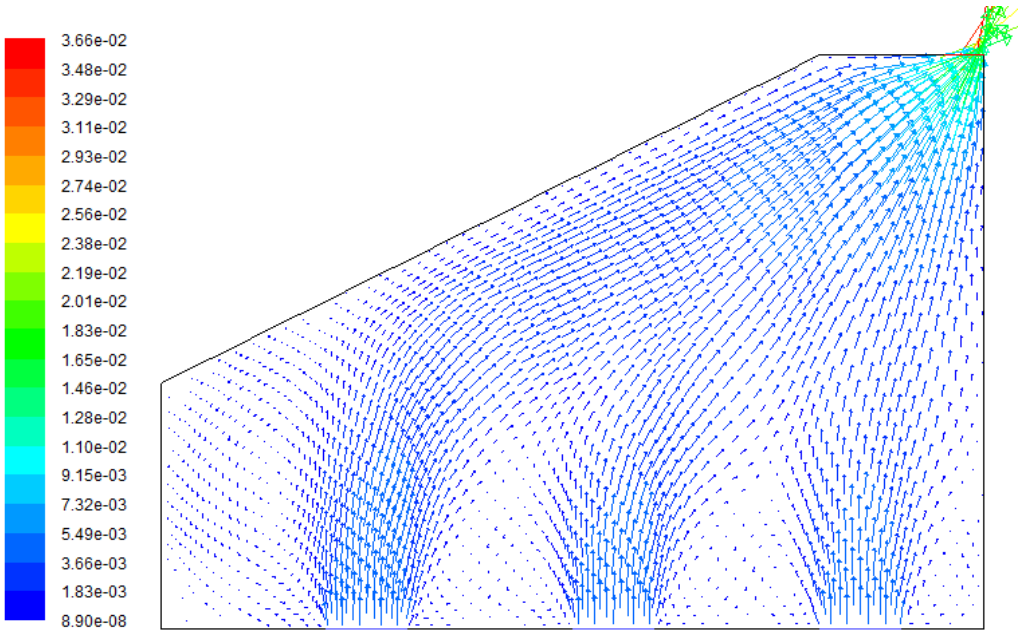

Figure (9): . Velocity vectors for LOC-BT configuration of the dryer.

One reason for the large variation in the flow fields for different locations is due to the fact that the inlet vents are more in LOC-BT configuration whereas it is single unit in the case of LOC-FR. This is because a two-dimensional domain has been considered. If a full three-dimensional domain is to be considered, then the inlet vents in LOC-FR could be more, which would improve the characteristics of the flow field. A three-dimensional study however would need huge computational resources and modeling, which could be taken in future.

5 Conclusions: Numerical modeling of a direct type solar dryer was performed and air flow and temperature distribution inside the dryer chamber was analyzed. The computational domain considered was two-dimensional. The study focused on the effect of locations of the inlet and outlet vents on the flow field and temperature field inside the chamber, all other conditions remain same. It can be concluded that air flow and temperature distributions are more uniform when the inlet vents are placed at the bottom wall and outlet vent is place at the top wall of the drying chamber. Moreover, a three dimensional analysis can be done to obtain more detailed information on the air flow and temperature distribution.

References:

[1] A. Fudholi, K. Sopian, M. H. Ruslan, M. A. Alghoul, M. Y. Sulaiman, Renewable and Sustainable Energy Reviews, 14 (2010) 1-30.
[2] M. A. Leon, S. Kumar, S. C. Bhattacharya, Renewable and Sustainable Energy Reviews, 6 (2002) 367 – 393.
[3] S. Singh and S. Kumar, Solar Energy, 86 (2012) 87-98.
[4] P. S. Chouhan, A Kumar, P. Tekasakul, Renewable and Sustainable Energy Reviews, 51 (2015) 1326 - 1337.
[5] Y. Amanlou and A. Zomorodian, Journal of Food Engineering, 101 (2010) 8-15.
[6] ANSYS FLUENT®, User's Guide", Release 12.0.
[7] C. B. Maia, A. G. Ferreira, L. C. Gomez, S. de M. Hanriot, T. de O. Martins, Int. J. Research and Reviews in Applied Sciences, 10/3 (2012) 382 – 389.

*****